Swansea University
Prifysgol Abertawe

Cronfa
Setting Research Free

Cronfa - Swansea University Open Access Repository

This is an author produced version of a paper published in:
Journal of Applied Physics

Cronfa URL for this paper:
http://cronfa.swan.ac.uk/Record/cronfa43487

Paper:
Abdelaziz, A., Ishijima, T. & Tizaoui, C. (2018). Development and characterization of a wire-plate air bubbling plasma for wastewater treatment using nanosecond pulsed high voltage. *Journal of Applied Physics, 124*(5), 053302
http://dx.doi.org/10.1063/1.5037107

This item is brought to you by Swansea University. Any person downloading material is agreeing to abide by the terms of the repository licence. Copies of full text items may be used or reproduced in any format or medium, without prior permission for personal research or study, educational or non-commercial purposes only. The copyright for any work remains with the original author unless otherwise specified. The full-text must not be sold in any format or medium without the formal permission of the copyright holder.

Permission for multiple reproductions should be obtained from the original author.

Authors are personally responsible for adhering to copyright and publisher restrictions when uploading content to the repository.

http://www.swansea.ac.uk/library/researchsupport/ris-support/

Development and characterization of a wire-plate air bubbling plasma for wastewater treatment using nanosecond pulsed high voltage

Ayman A. Abdelaziz[a*1], Tatsuo Ishijima[b], Chedly Tizaoui[a*]

[a] Centre for Water Advanced Technologies and Environmental Research, College of Engineering, Bay Campus, Swansea University, Swansea SA1 8EN, UK

[b] Research Center for Sustainable Energy and Technology, Kanazawa University, Kakuma-machi, Kanazawa, Japan

Corresponding author: Ayman A. Abdelaziz (AA) & C. Tizaoui (CT) E-mail:.a.abdelaziz@science.au.edu.eg (AA) & c.tizaoui@swansea.ac.uk (CT) Tel.: +44(0)1792606841

Abstract

This study developed a prototype of wire-plate air bubbling plasma reactor that can be easily scaled up for wastewater treatment. The electrical characteristics, including the discharge current and average power consumed, of the developed reactor were deeply investigated at different operating parameters and solution conductivities. The performance of the reactor was examined on the basis of energy efficiency and methylene blue (MB) decoloration efficiency. Moreover, the removal of the Total Organic Carbon (TOC) and the changes of the physicochemical properties of solution, including pH, conductivity and temperature were evaluated. The analysis of current discharge and average power consumed showed that the discharge mode in the present reactor is a filamentary streamer. Interestingly, the solution conductivity had no effect on the average power consumed at low applied voltages, due to confinement of the discharge in a small area surrounding the discharge electrode in the gas phase. However, at relatively

[1] Physics Department, Faculty of Science, Assiut University, Assiut, Egypt.

high voltages, the effect of conductivity on the average power consumed was noticeable, yet it had no effect on the decoloration efficiency at the same average power. The present reactor showed a high energy efficiency value of 42 g/kWh at 50% decoloration of 30 mg/L MB solution, but it dropped to 14 g/kWh at 97% decoloration. A first-order kinetics model described well the decoloration reaction rates and the overall rate constant correlated linearly to the average power.

Keywords: Air Bubbling Plasma; Pulsed Discharge; Nonthermal Plasma; Wastewater Treatment; Energy Efficiency.

1. Introduction

Over the last two decades, nonthermal plasma (NTP) has been investigated intensively as an advanced oxidation process for water and wastewater treatment [1-4]. This interest in NTP is due to the varieties of chemical and physical processes that develop in NTP to produce mixtures of chemical reactive species (e.g. $^{\bullet}OH$, $^{\bullet}O$, H, HO_2, H_2O_2, O_3, NO, NO_2), strong electric field, shock waves and intense UV radiation [5], which are difficult to obtain in ordinary oxidation methods. Owing to their strong oxidation ability, these reactive species can directly attack and oxidise organic pollutants and inactivate microorganisms contained in wastewater [6, 7]. Various NTP techniques have been developed and examined for water purification [8-13]. These techniques can be classified, according to the location and the distribution of the discharge with respect to the water, to three main categories [14]; direct discharge in water (liquid phase), discharge over the water surface (gas phase), and bubbling discharge (gas-liquid interphase). Each of these techniques displayed certain advantages and disadvantages. In the direct discharge in water, the plasma generated has sufficient contact with the

liquid phase, which is crucial for immediate supply of the short-lived reactive species (such as •OH) in the solution. However, high electric field in the order of several MV/cm is required to initiate the discharge inside the water [15]. In addition, this method of discharge always suffer from discharge electrode corrosion and is affected by the solution conductivity [16], as the current may transmit through the water causing energy wastage and rapid heating. Techniques of generating plasma above the water surface are used effectively in water treatment because they require simple electrode shapes and are convenient for use [17]. It was found that the discharge in air consumes approximately a factor of 10 less energy than in water [17, 18]. However, this method cannot be applied to treat a large volume of water due to the slow penetration (diffusion) of the reactive species in the treated water. Therefore, the combination of liquid phase and gas phase discharge processes showed more synergistic effect [19] which increased the energy efficiency of the treatment process [20]. For this purpose, several techniques for bubbling plasma discharge in water using various bubbling gases and voltage regimes have been developed and studied recently [21-28], for . These techniques showed a greater production of the reactive species and a highly efficient wastewater treatment. In the bubbling plasma discharge technique, the reactive species are first generated in the gas phase, to avoid the high electric field required for the direct discharge in water, and are then immediately transferred to the treated water through the generated bubbles. By doing this, the mass transfer of the reactive species into water is enhanced, which leads to improved reactor performance. Moreover, generating plasma in bubbles inside the water allows producing various kinds of chemical reactive species in the gas phase as well as in the liquid medium. However, upscaling and energy efficiency are still some of the challenges to address in these reactors. Takahashi *et al* [29, 30] presented a new bubbling plasma-based reactor, which can be extended to treat a large volume of water.

However, they only spotlighted on the effect of the operating conditions, including the applied voltage and the solution conductivity, on the generation of the reactive species and the decoloration efficiency of dyes (indigo carmine, acid Red 1 and acid blue 74) and some organic pollutants (1,4-dioxane) without focusing on the effect of these parameters on the electrical characteristics and their impact on the treatment process. To optimize and be able to scale up the reactor to treat large volumes of wastewater, it is however necessary to understand the effect of the operating parameters and the solution properties on the electrical characteristics of the reactor.

Thus, in this study, a prototype bubbling plasma-based reactor is developed and its electrical characteristics are investigated deeply as a function of the operating conditions, including the applied voltage, the frequency, and the solution conductivity. The main feature of this reactor is that it is easy to build and upscale to treat a large volume of wastewater. The performance of the reactor was evaluated through the decoloration of methylene blue (MB), as a model of organic contaminants in water. In order to achieve high-energy efficiency, a pulsed voltage with short pulse width is used in this study. The important consequence of the short pulse width of the applied voltage is the minimisation of the power dissipated in the acceleration of ions, due to their low mobility, which do not contribute to the dissociation processes of the water and the pollutant molecules [18, 31, 32]. Finally, to get a better understanding of the performance of this reactor in wastewater treatment, the effects of plasma on TOC and the physicochemical characteristics of solution were evaluated.

2. Experimental details

Figure 1 (a) shows the schematics of the experimental setup used in the present study. The reactor consists of a water tank made from an acrylic rectangular cuboid (with

internal dimensions 40 mm depth, 80 mm width, and 80 mm length) containing a plasma source. The plasma source consists of a perforated acrylic tube with an inner diameter of 4 mm, a thickness of 1 mm, and length (the actual length inside the reactor) of 80 mm inserted inside the water tank at its bottom, as shown in figure 1 (b and c). A 0.5-mm diameter tungsten electrode placed along and at the center of the perforated acrylic tube was used as a discharge electrode, from which the plasma was emitted. The structure of this reactor provides an easy way to replace the perforated tube and the discharge electrode with a larger one when a treatment of large volume is required. A stainless steel plate submerged in the solution at 9 mm beside the acrylic tube was used as a ground electrode. In order to generate plasma along the water tank, the carrier gas (dry air) was fed to the acrylic tube at a constant flow rate of 2 L/min (controlled by a gas flow controller (FC)), and it was introduced into the solution as bubbles through 10 holes uniformly distributed horizontally on the acrylic tube. The diameter of each hole was 0.8 mm. All experiments reported in this study were performed at a constant volume of solution (170 mL).

The applied voltage to the reactor has pulse waveform generated by a HV pulser (Suematsu Elect. Co., Ltd, Japan), 500 Hz (variable), 30 kV (variable), 50 ns fixed rise time, and 100 ns fixed pulse width. The high voltage pulser has a unique feature of producing nanosecond pulse voltage with short and fixed pulse width. The applied voltage was measured using a high-voltage probe (Tektronix P6015A, 40 kV, 75 MHz, 1000X), which was connected to a digital oscilloscope (Tektronix MDO 3024, 200 MHz, 2.5 GS/s). The current through the reactor was measured using a Pearson current monitor (model 4997) and displayed using the digital oscilloscope.

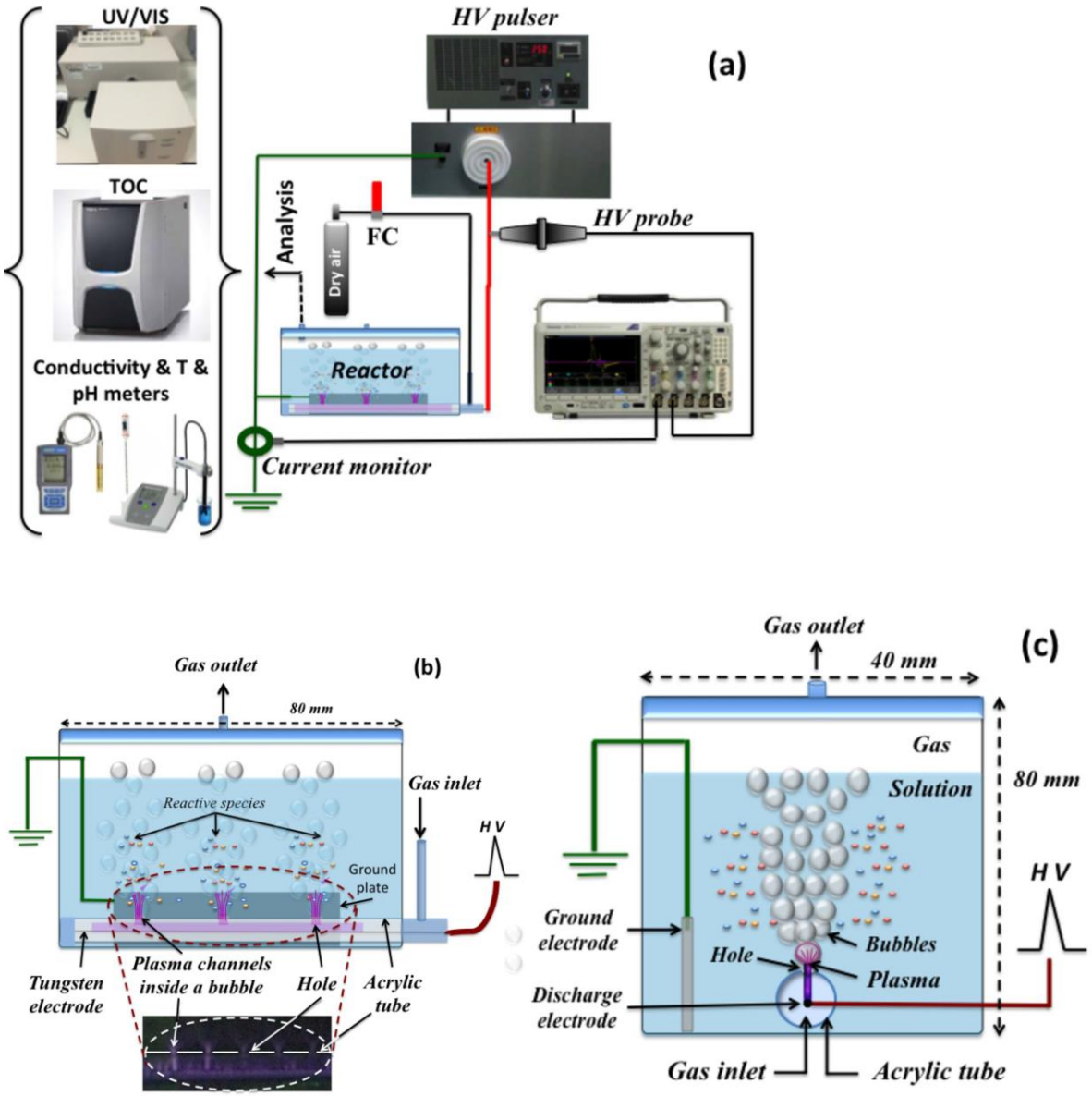

Fig. 1 Schematics of (a) the experimental setup, (b) side of the reactor (for simplification, only 3 holes in the acrylic tube are used in the drawing) and (c) cross section of the reactor

Analytical grade methylene blue (MB) in powder form (Fisher scientific, UK) was used to prepare 100 mg/L stock solutions in deionized water. From the stock solution, the required concentrations of MB were prepared by dilution in deionized water. Analytical grade sodium chloride (NaCl) was used to adjust the conductivity of the solution from 1 μS/cm to 1000 μS/cm.

A UV/Vis spectrophotometer (Agilent, 8453) was used to determine the concentration of MB solutions using a calibration curve determined at maximum absorbance wavelength of 664 nm. The decoloration efficiency percentage was determined by the following equation:

$$\eta_d\ (\%) = \frac{C_0 - C}{C_0} \times 100 \qquad (1)$$

where C_0 is the initial concentration of MB (mg/L) and C is the concentration after different discharge times.

The energy efficiency of the degradation process is determined by the following equation:

$$Y\left(\frac{g}{kWh}\right) = \frac{C_0 \times v \times \eta_d \times 10^{-6}}{P_{\mathrm{av}} \times t \times 100} \qquad (2)$$

where v (L) is the volume of the aqueous solution, t (h) is the treatment time, and P_{av} (kW) is the average power consumed, which was calculated using the following equation:

$$P_{\mathrm{av}} = f.\mathrm{E}_{\mathrm{av}} \qquad (3)$$

where f and E_{av} are the driven frequency and the consumed energy in the reactor, respectively. The consumed energy E_{av} in the reactor was calculated based on the time integration of the product of the voltage and current waveforms over the pulse duration (one cycle) using the following equation:

$$E_{\mathrm{av}} = \int_0^{\tau} V(t) \cdot I(t) dt \qquad (4)$$

where V(t), I(t), and dt are the instantaneous values of the applied voltage, current, and the sample interval, respectively, which were recorded by the oscilloscope. τ is the period of the applied voltage.

The Total Organic Carbon (TOC) of the solution was measured by a TOC Analyzer (TOC-L, Shimadzu) using the combustion catalytic oxidation coupled with infrared detection method. The TOC content was determined from the difference of total carbon and total inorganic carbon measurements and its reduction efficiency in percentage was calculated using the following equation:

$$\eta_{TOC}\ (\%) = \frac{(TOC)_0 - (TOC)}{(TOC)_0} \times 100 \qquad (5)$$

where $(TOC)_0$ and (TOC) are the concentrations of TOC (mg/L) before and after the plasma treatment, respectively. The conductivity (σ) and the pH of the solution were measured by a conductivity meter (Oakton Waterproof CD650 Multiparameter Meter Kit) and a Five Easy pH meter (Mettler Toledo, UK), respectively.

3. Results and discussion

3.1. Characteristics of the air-bubbling plasma reactor

3.1.1. Plasma characteristics

Figure 2 shows photos of the plasma generated in the reactor at different applied voltages when the frequency was 300 Hz, and solution conductivity was 1 μS/cm. As it can be seen in the figure, after the onset voltage (discharge inception) value, the plasma is ignited and takes place around the discharge electrode inside the acrylic tube. With increasing the applied voltage, the plasma volume is increased over the upper side of the discharge electrode. However, the discharge along the discharge electrode was distributed non-uniformly, where the plasma channels were denser and longer at some locations in the discharge electrode corresponding to the holes of the acrylic tube. This is due to the

differences in conductivity and the permittivity between water and the acrylic tube, which leads to concentrated and enhanced electric field on these holes. Figure 2 also shows that the higher the applied voltage, the longer the plasma channels at the holes of the acrylic tube. With increasing the applied voltage, the plasma channels became long enough to exit the holes to the solution through the bubbles. Further increase in the applied voltage made the plasma channels denser, which explains the increased brightness of the plasma as the voltage increased from 8 kV to 14 kV (figure 2). Figure 2 also shows that the brightness of the plasma channels inside the acrylic tube and in between the holes increases with increasing the applied voltage.

It should be mentioned that the discharge at the holes is pulsed corona discharge (PCD) due to the air gap between the discharge electrode and the water, while the discharge is dielectric barrier discharge (DBD) over the inside length of the acrylic tube excluding the holes. This means that the discharge in the present reactor consists of PCD at the holes and DBD in the remaining part of the acrylic tube body.

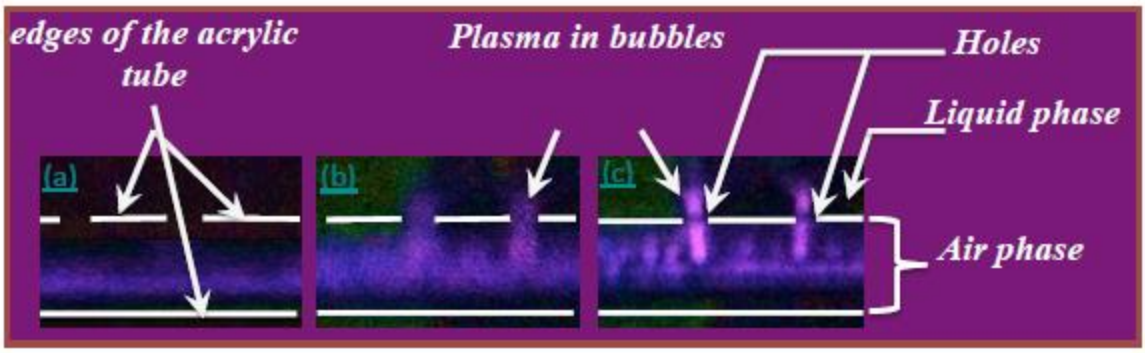

Fig. 2 Photos of the discharge as influenced by the applied voltage, f= 300Hz and σ_i=1 μS/cm (a) V_p≈ 8kV, (b) V_p≈12 kV, and (c) V_p≈14 kV

The typical waveforms of the pulsed voltage applied to the reactor and the associated discharge current are shown in figure 3 at a frequency of 300 Hz, a peak applied voltage of V_p=13 kV, and solution conductivities of σ =50 and 1000 μS/cm, respectively. The

discharge current appears in the form of series of narrow pulses. The amplitude of the highest current pulse was about 21 A, and the average power corresponding to this condition was 1.3 W. These current pulses indicate that the discharge was ignited in the reactor in the form of filamentary streamers, which resulted from the PCD at the holes and the microdischarges that were distributed over the internal surface of the acrylic tube. This observation of the discharge current is different than that observed using pin-holes needle electrodes submerged in aqueous solution [33] and over the surface of a treated solution [34, 35], where the discharge current consisted only of one peak instead. At this experimental condition, the applied voltage waveform shows small peaks of the applied voltage associated with the main peak voltage. Although the amplitudes of these peaks are less than the onset voltage value, current pluses were observed. This indicates that the microdischarges of the filamentary streamers from the main discharge (ignited at the main peak voltage) are accumulated over the inner surface of the acrylic tube [26] and leads to enhance the applied voltage of the associated peaks to simulate the discharge re-ignition.

Figure 3 also shows that the solution conductivity (50 and 1000 μS/cm) has no significant influence on the shape of the applied voltage. This is due to the characteristics of the power supply used in this study, where the delivered voltage is independent of the load. Although the filamentary mode of the discharge remained at high conductivity (1000 μS/cm), the amplitude and the density of current pulses are higher. This is could be explained by the fact that the higher solution conductivity conducts electricity more than the solution with a low conductivity, due to the high concentration of the positive and negative ions in the solution that can migrate easily under the effect of an electric field, leading to increased current [5, 33, 36, 37].

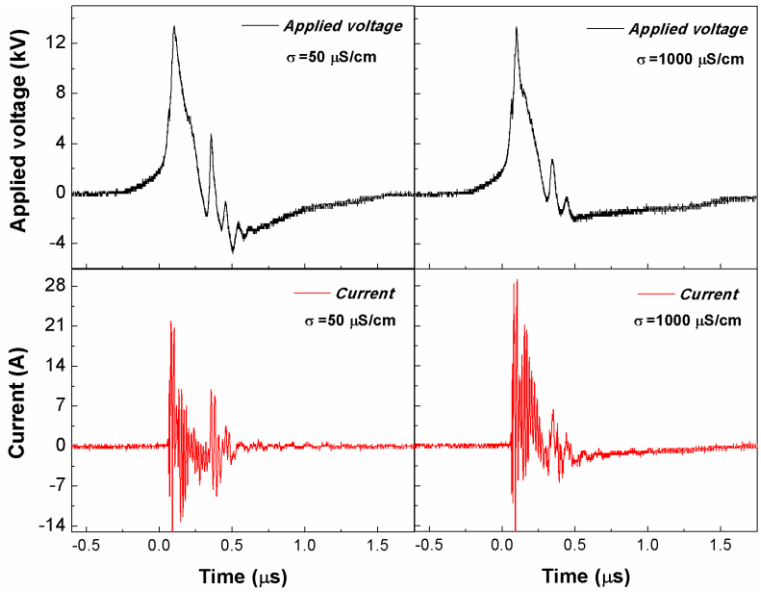

Fig. 3 *Current–voltage waveforms of the plasma at peak applied voltage of 13 kV, frequency of 300 Hz, and different conductivities (σ_i=50 and σ_i=1000 μS/cm)*

3.1.2. Effect of pulse frequency

The average power consumed in the reactor as a function of the frequency at different applied voltages is shown in figure 4. As can be observed, the average power consumed increased linearly with increasing the frequency, a similar behavior for the average power consumed was found in [38] using DBD immersed in water. This observation indicates that the energy dissipated per cycle is independent of the driven frequency and it is constant, at our experimental range of frequencies, as long as the applied voltage is constant, as shown in the inserted figure in figure 4.

On the other hand, the average power consumed in the reactor increased nonlinearly with the applied voltage at the various frequencies, as shown in figure 5.

The data of the average power consumed versus the applied voltage is fitted by an empirical equation that correlates the average power consumed to the frequency and the peak voltage, as shown in the following formula;

$$P_{\mathrm{av}} = A(V - B)^2 \qquad (5)$$

where *A* and *B* are constants. Interestingly, the constant A was found to be a function of the frequency ($A=3\times10^{-5} f$). This behavior of the average power consumed in the current reactor is similar to that obtained in surface DBD [39, 40]. This similarity might be referred to the DBD behavior of the present reactor.

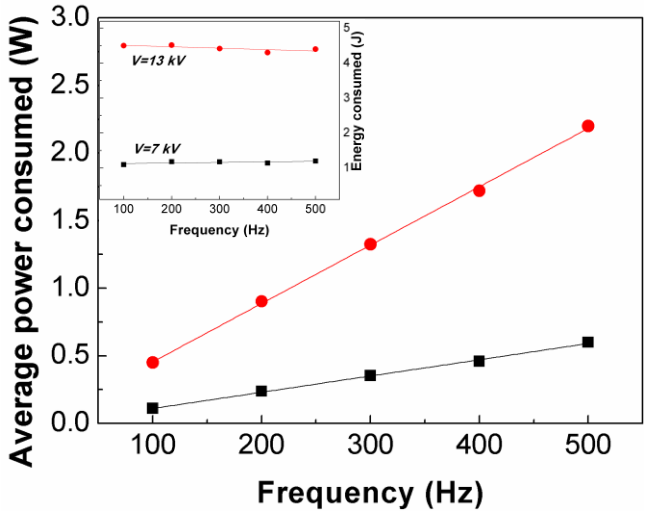

Fig. 4 Average power consumed in the reactor as a function of the frequency at different peak applied voltages (7 kV and 13 kV) and σ_i=50 µS/cm. The insert shows the relationship between the energy consumed and the frequency.

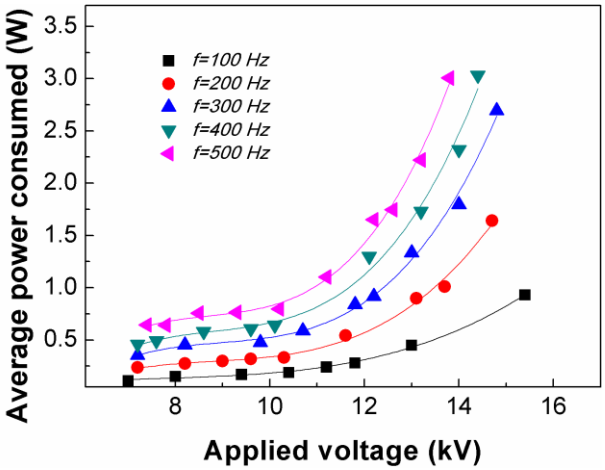

Fig. 5 Average power consumed in the reactor as a function of the peak applied voltage at different frequencies and σ_i=50 µS/cm

3.1.3. Effect of solution conductivity

Figure 6 depicts the dependence of the average power consumed in the reactor on the conductivity of the solution at different applied voltages and a constant frequency of 300 Hz. What is striking in this figure is that the average power consumed in the reactor was independent of the solution conductivity at relatively low applied voltage, while it was remarkably dependent on the solution conductivity after a certain applied voltage V_e (V_e ~11 kV in this experimental condition). The general trend of the effect of the conductivity on the average power consumed after V_e is very similar to that found in [41], using an alternative current-capillary discharge in water. This phenomenon can be explained by increased solution conductivity which lead to enhanced and concentrated electric field on the holes resulting in intensifying the discharge inside the bubbles. The enhancement of the electric field on the holes with increasing the water conductivity is due to reducing its resistivity [30], which leads to increased voltage drop between the water surface and the discharge electrode for the same applied voltage between the discharge electrode and the grounded stainless steel plate. However, at a relatively low applied voltage, there is no effect of the solution conductivity on the discharge due to the confinement of the discharge around the discharge electrode in the gas phase inside the acrylic tube, as described above. The effect of the solution conductivity started to be noticeable when the discharge channels are long and strong enough to reach and penetrate the liquid phase under voltages equal to and higher than V_e. This is supported by figure 3, where the current increased at high conductivity and applied voltage. This explanation is supported also by measuring the onset voltage of the discharge at the different solution conductivities, where the onset voltage was approximately independent of conductivity in the range of σ= 1– 1000 μS/cm, a similar behavior was also obtained by Šunka et al [37] using needle-plate electrodes immersed in water.

It is noteworthy to mention that the variation of the distance between the discharge electrode and the ground electrode (3 – 12 mm beside the acrylic tube) had no effect on the discharge characteristics, including the average power consumed, under the investigated conditions (high conductivity and applied voltage).

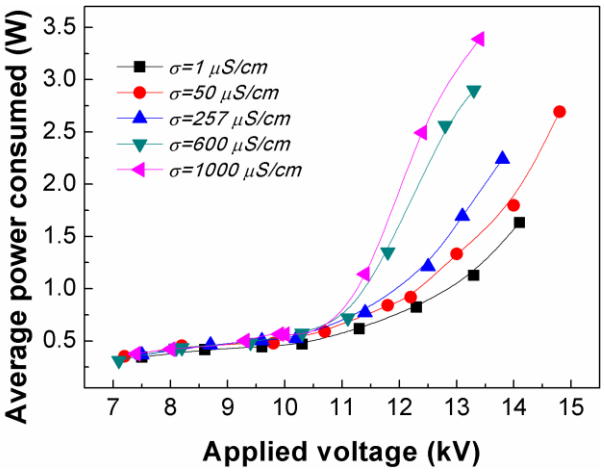

Fig. 6 Average power consumed in the reactor as a function of the peak applied voltage at different conductivities and f=300 Hz

3.2. Decoloration of MB solutions

3.2.1 Decoloration and energy efficiencies

Figure 7 demonstrates the effect of the averaged power consumed on the decoloration efficiency of the MB solution, where the initial concentration of the MB was 10 mg/L, the conductivity of the solution was 1 μS/cm, and the initial pH of the solution was 5.6. As can be seen in figure 7, the decoloration efficiency increases with increasing the treatment time at our investigated range of the powers. The increase of the decoloration efficiency was very rapid at the beginning of the treatment and followed by a slow increase at a longer treatment time. In addition, the decoloration efficiency increases with increasing the average power consumed.

Since the discharge is ignited in air, the energetic electrons generated collide with the background gaseous molecules (such as O_2 and N_2) to produce primary gas-phase reactive species, such as $^{\bullet}OH$, $^{\bullet}O$, H, O_3, $^{\bullet}N$, NO, NO_2 and ions [42, 43]. These reactive species, in turn, are transferred into the aqueous solution via the bubbles to react with the MB molecules and generate secondary aqueous-phase reactive species [44-46], such as H_2O_2, $^{\bullet}OH$, O_3, NO_x, HNO_2, and HNO_3. Therefore, the decoloration of the MB in the reactor results from the simultaneous contribution of numerous different reactions driven by the primary and secondary reactive species. As the power increases, the electrons gain much energy and induce more reactive species [47, 48], which benefits the decoloration efficiency. That is why the higher the average power consumed, the higher the decoloration efficiency and the shorter the treatment time (figure 7). The decoloration efficiency of 95.7% was achieved after 10 min of the treatment at P_{av}=1.13 W, while only 93.6% of decoloration efficiency is attained after 20 min of the treatment at P_{av}= 0.42 W. On the other hand, the energy efficiency of the decoloration process decreased with increasing the average power consumed, as shown in figure 8. Although increasing the power consumed is associated with more and longer plasma channels, figure 8 indicates that much power is dissipated in the reactor at the relatively high input power. The loss of the energy efficiency at the high input power could be due to: (1) increased plasma temperature, due to increased plasma channels, causing destruction of certain useful reactive species for MB decomposition, such as ozone [49, 50]; (2) increased compensated space charges on the channels head by ions present in the solution [37] when the plasma channels are penetrated into the solution, (3) increased Ohmic loss with increasing the penetration of the plasma channels into the solution [30].

The highest energy efficiency obtained was 27 g/kWh when the decoloration efficiency was 55%, and it decreased to 11.4% when the decoloration efficiency was 93.6% at the same power consumed and initial MB concentration. It is worth mentioning that this value of the energy efficiency is much higher than that reported for the decoloration of MB solutions of characteristics close to our study but using different plasma techniques such as plasma jet (0.4 g/kWh at ~ 88% decoloration) [51] pulsed corona discharge (4.6 g/kWh at 91% decoloration) [52] over solution surface, pulsed corona discharge in gas bubbles (5 g/kWh at 90% decoloration) [46], microwave plasma (0.12 g/kWh at 96.56% decoloration) [53] and DC corona discharge (1.2 g/kWh at 95.7% decoloration) [54] in solution, and Ar bubbling discharge (~0.8 g/kWh at ~100% decoloration) [55].

The fast increase in the decoloration efficiency at the beginning of the treatment indicates that the reactive species are utilized efficiently in the decoloration process due to the high concentration of MB available in the solution. This explains the increase in the energy efficiency at the beginning of the treatment, figure 8. The rather slow increase in the decoloration of the MB at longer treatment time is related to the low concentration of the MB molecules in the solution, which increase the possibility of consuming the generated reactive species to (1) form further reactive species (e.g. nitrogen oxides that reduce the $^{\bullet}OH$ and O_3 concentration [44]) undesirable for the decoloration of the MB or (2) react with the intermediate byproducts rather than react with the MB molecules.

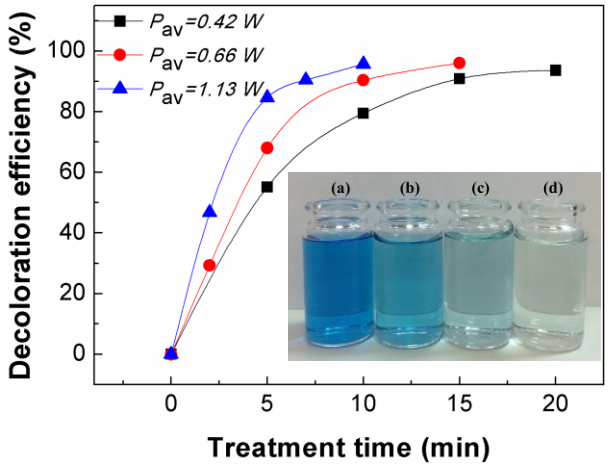

Fig. 7 Decoloration efficiency of the MB as a function of the treatment time at different powers, f=300 Hz, $pH_i \approx 5.6$ and $\sigma_i \approx 1$ μS/cm. The insert shows the color change of the MB solution before and after plasma treatment at P_{av}=0.66 W, C_0=10 mg/L, $\sigma_i \approx 1$ μS/cm and different treatment times (a) 0 min, (b) 5 min, (c) 10 min, and (d) 15 min

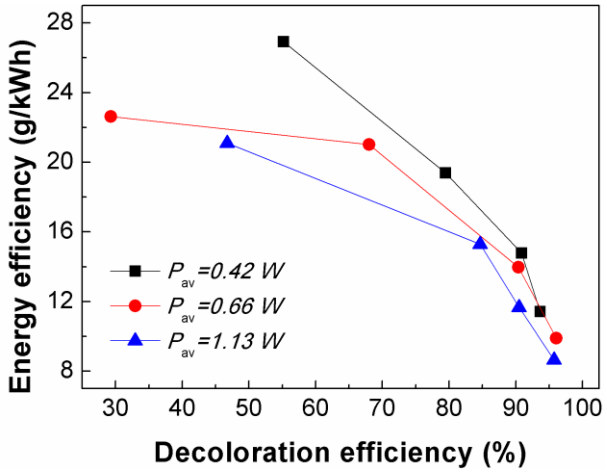

Fig. 8 Energy efficiency of the decoloration process of the MB at different powers, f=300 Hz, C_0=10 mg/L, $pH_i \approx 5.6$ and $\sigma_i \approx 1$ μS/cm

3.2.2. Reaction kinetics

The overall decoloration process proceeds via simultaneous complex reactions involving several reactive species (e.g. O_3 and $^{\bullet}OH$) to produce intermediate products and ultimately H_2O and CO_2 if the reaction is extended for a long time. The decoloration

reaction rate may be described by a second-order reaction model (i.e. $r_i = k_i C_{Ai} C$) [56], where A_i refers to reactive species i, k_i is the second order reaction rate constant relative to A_i, C_{Ai} is the concentration of reactive species i and C is the concentration of MB. Given that these reactive species are continuously produced by the plasma and supplied to the solution, their concentrations in solution may be assumed constant. Consequently, the overall reaction rate of MB decoloration, r_{MB}, may be described by a first-order reaction kinetics (i.e. $r_{MB} = k_{overall} C$) where $k_{overall} = \Sigma k_i C_{Ai}$ is the first-order overall reaction rate constant. The classical linearized form of a first-order reaction rate (i.e. $-ln(C/C_0) = k_{overall}.t$; where t is time and C_0 is the initial MB concentration) was applied to fit the experimental data, obtained at different average powers, and the results are shown by dash lines in figure 9. The figure shows good agreement between the experimental data and the model indicating that the first-order kinetics is suitable to describe the decoloration of MB in the wire-plate air bubbling reactor developed in this study. The values of the overall first-order reaction rate constant were obtained from the slopes of the straight lines shown in figure 9 and were plotted as a function of the average power as displayed in the inset figure of figure 9. According to the inset figure, as the average power, P_{av}, increased, $k_{overall}$ has also increased linearly which suggests that $k_{overall}$ could be correlated to P_{av} by a linear relationship of the form $k_{overall} = \alpha P_{av}$; where α is a constant. The constant α was determined from the slope of the line in the inset figure and its value was found equal to 0.30 $min^{-1}.W^{-1}$. In previous studies on aqueous dye decoloration using plasma discharge, the kinetics of the reaction was also described by a first-order reaction rate model [45]. The values of the first-order rate constants obtained in the present study are in the order of 2 to 3 times higher than those reported in [45] at similar power levels. This indicates that the reactor developed in this study was more efficient to generate higher concentrations of reactive species.

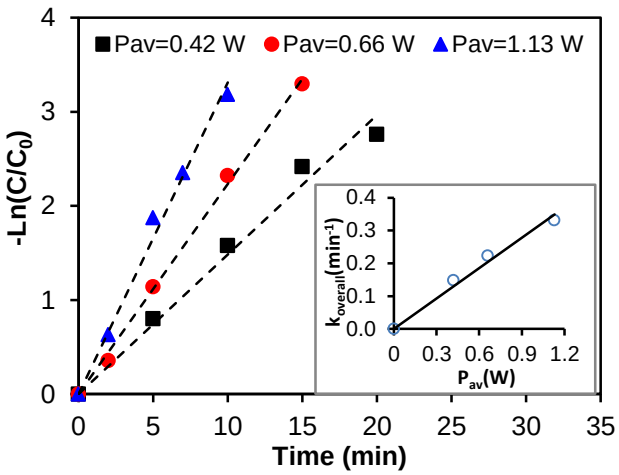

Fig. 9 Kinetics of the decoloration of MB at different powers, f=300 Hz, C_0=10 mg/L, pH_i≈5.6 and σ_i≈1 µS/cm. The insert shows the relation between the average power consumed and the first-order reaction rate constant.

3.2.3. Effect of solution conductivity

The dependence of the decoloration efficiency and the energy efficiency on the conductivity of the solution at a constant average power consumed is shown in figures 10 and 11, respectively. Given that the energy efficiency increases at low input power (figure 8), this experiment was conducted at a relatively reduced power (~0.88 W). It is apparent that the conductivities in the range of 1–1000 µS/cm have no influence on the decoloration process, the decoloration efficiency and the energy efficiency, of the MB at the same average power consumed. These results are in qualitative agreement with those obtained in [13, 30, 44, 57] using bubbling discharge based reactors, where the solution conductivity had no significant effect on both the degradation efficiency of the model pollutants used and the reactive species generated. This is because the plasma, at this selected value of the average power consumed, was mainly formed in the gas phase inside the dielectric tube and entered within bubbles into the aqueous solution. This indicates that the majority of the input power, at the relatively low value of the power consumed,

was used effectively in the production of the plasma, rather than dissipated in the solution as a load, due to the change of the solution conductivity. However, at high values of the power consumed, the size of the plasma channels might be high enough to penetrate the solution and affect and been affected by the solution conductivity. That is why the solution conductivity showed a significant effect in the cases of direct plasma discharge in water using DBD [48, 58], points-to-plane [59], and bubbling discharge (where the bubbles are introduced between two electrodes immersed in water) [31] based reactors, due to compensation of the space charge on the head of plasma streamers by the ions presented in the solution, which led to a decrease in the streamer length [37], and subsequently decreasing the reactive species in the bulk solution [60]. This suggests that bubbling plasma discharge based reactor would exhibit a good prospect for wastewater treatment.

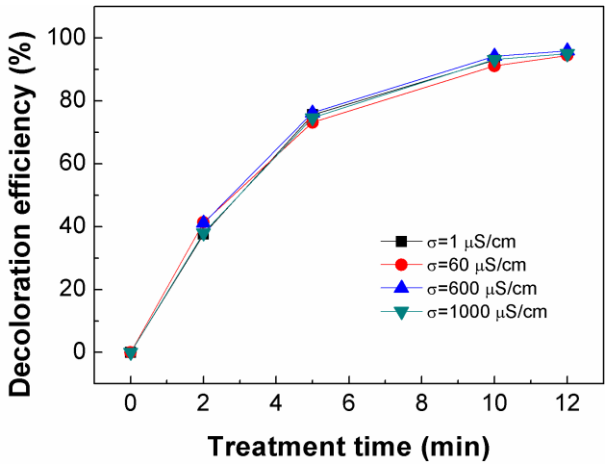

Fig. 10 Decoloration efficiency of the MB as a function of the treatment time at different solution conductivities, P_{av}=0.88 W, $pH_i \approx 5.6$, C_0=10 mg/L, and f=300 Hz

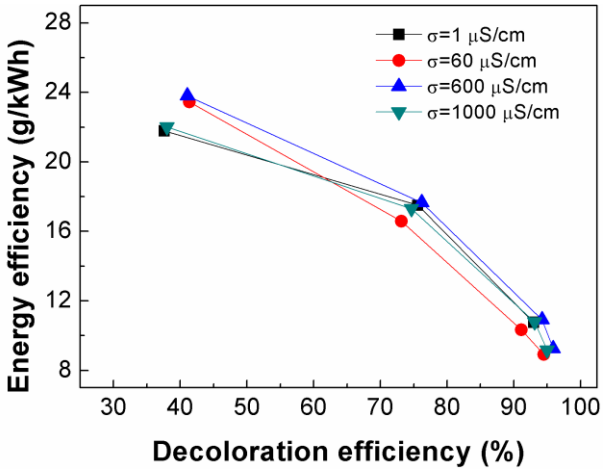

Fig. 11 Energy efficiency of the decoloration process of the MB at different solution conductivities, P_{av}=0.88 W, pH_i≈5.6, C_0=10 mg/L, and f=300 Hz

3.2.4. Effect of MB initial concentration

The performance of the reactor was also evaluated to decolorate different concentrations of MB at the same average power consumed of P_{av}=0.66 W and the same initial solution characteristics (pH= 5.6 and conductivity=1 mS/cm), as shown in figure 12. It can be seen that the effect of the initial concentration of MB on the decoloration efficiency is noticeable only at relatively high concentration and the effect was more pronouncing at the beginning of the treatment time, where the decoloration efficiency decreased at 5 min from 72% to 68% as the initial concentrations of MB were increased from 5 mg/L to 10 mg/L, and it decreased abruptly to 47.7% when the initial concentration increased to 30 mg/L. At relatively long treatment time, the difference in the decoloration efficiency was less pronounced, where the decoloration efficiency decreased at 15 min of the treatment time from 96% to 89.7% as the initial concentrations of MB was increased from 10 mg/L to 30 mg/L. This is could be due to two reasons: (1) increasing the number of the reactant molecules in the reaction [51], (2) the primary reactive species in the gas phase react with the water molecules as well as with the MB molecules and the degradation byproducts, as it was described above. These primary reactive species produced in the

reactor were maintained at a specific concentration at a fixed applied voltage and input power [3, 61]. However, more secondary reactive species would form at a lower concentration of MB due to the higher chance of the reaction between the primary reactive species and the water molecules resulting in increasing the secondary reactive-species and subsequently increasing the degradation efficiency at the low initial concentration of MB. Further investigations including measurements of the secondary reactive species during the decoloration process are needed to confirm this suggestion.

On the other hand, the energy efficiency of the decoloration process depends obviously on the initial concentration of MB, as shown in figure 13. For all the concentrations, the energy efficiency decreased with increasing the decoloration efficiency, while it increased with increasing the initial concentration of MB. Similar behavior was also reported for the degradation of MB [45] and for 17β-Estradiol in aqueous solutions using DBD based reactors [62]. This indicates that the present reactor has the ability to decolorise large amounts of MB with high energy-efficiency. This also indicates that the deposited energy to the reactor would be used more efficiently when the initial concentration of the MB is high, due to the higher opportunities of reacting the reactive species with the MB molecules at high MB concentrations.

The maximum energy efficiency obtained in this study was 42 g/kWh at 50% of the decoloration efficiency of 30 mg/L, and the energy efficiency corresponding to 97% of the decoloration efficiency for MB initial concentration of 30 mg/L was about 14 g/kWh.

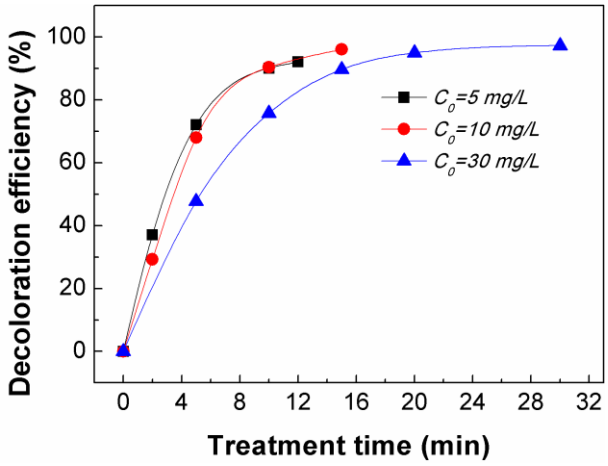

Fig. 12 Decoloration efficiency of the MB as a function of the treatment time at different MB initial concentrations, P_{av}=0.66 W, f=300 Hz, $pH_i \approx 5.6$ and $\sigma_i \approx 1$ µS/cm

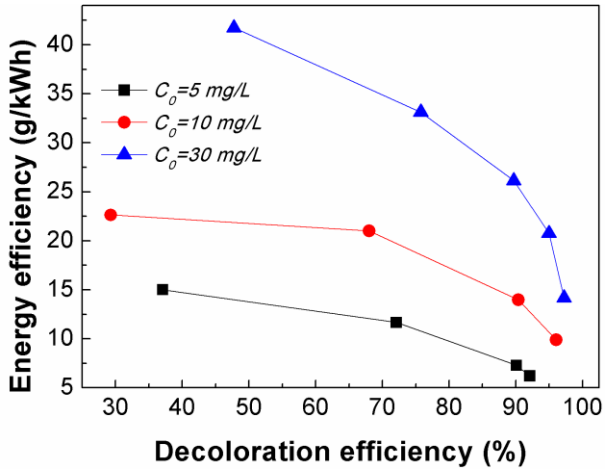

Fig. 13 Energy efficiency of the decoloration process of the MB at different initial MB concentrations, P_{av}=0.66 W, f=300 Hz and $\sigma_i \approx 1$ µS/cm

3.3 TOC measurements

Measurements of the Total Organic Carbon (TOC) during the treatment process are important. This is not only because TOC is an index of pollutant content in the solution, but its variation depicts the extent of mineralization during the treatment process. In an oxidation process, the decomposition of organic compounds may lead to organic acids such as carboxylic acids and formic acids [50] as intermediates which accumulate in solution due to their low oxidation reaction rate constants. The complete mineralization to CO_2 of these intermediates becomes difficult and, as a result, longer treatment times or

harsher oxidation conditions will be required to achieve higher TOC reductions. In this study, TOC reduction efficiency was determined at different treatment times using an initial MB concentration of 10 mg/L and an average power 1.13 W. The results showed little TOC reduction efficiency of about 15% during 30 min treatment time. The low reduction in TOC may be explained by the accumulation of oxidation intermediates (e.g. organic acids) that are harder to further oxidise. Data presented in [63] also shows the similar level of TOC reduction (~20%) after 30 minutes degradation of Alizarin Red dye in dielectric barrier discharge plasmas. Despite achieving a relatively high energy efficiency in this study, the solution TOC remained high. Longer treatment times, therefore, may be required to enhance the extent of mineralization of the solution.

3.4. Effect of plasma on solution characteristics (pH, conductivity, and temperature)

The discharge produced in air bubbles under water not only can produce radicals and neutral reactive species (such as H_2O_2, $^{\bullet}OH$, and O_3**)** but also it generates ions (such as NO_2^- and NO_3^-), which have effects on the physicochemical characteristics of the treated solution [64]. This is confirmed by increasing the conductivity of the solution during the treatment process, as shown in figure 14. However, the increase of the conductivity of the treated solution was fast at the relatively low power, while it became slow at the relatively high power. This is could be referred to the penetration of the plasma into the treated solution at the high input power, which results in lowering the production rate of the reactive species and increasing the dissipating power in the reactor. Thus, this figure confirms that the penetration of the plasma channels into the solution is not favored for the production of the reactive species and subsequently the energy efficiency of the decomposition process.

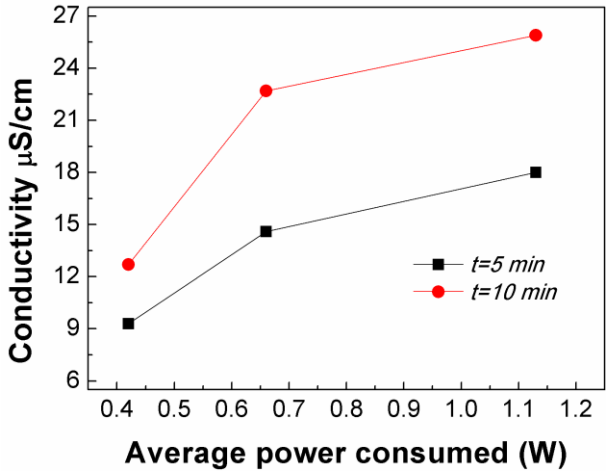

Fig. 14 Conductivity of the treated solution as a function of the treatment time at different powers, f=300 Hz, $pH_i \approx 5.6$ and C_0=10 mg/L

Figure 15 shows the change in the pH of the treated solution at different powers and at MB concentration of 10 mg/L. The figure shows that the pH decreases with increasing the treatment time and the decrease in the pH was rapid within the first 5 min of the treatment process then followed by a slow decrease. The decrease in the pH of the treated solution by the air bubbling plasma can be due to the following reasons:

(1) In air discharge, the excited nitrogen molecules undergo dissociation to form NO and NO_2 via the following reactions [49]:

$$N_2\,(A^3\Sigma_u^+) + O \rightarrow NO + N\,(^2D) \quad \text{(R1)}$$

$$N\,(^2D) + O_2 \rightarrow NO + O(^3P) \quad \text{(R2)}$$

$$N\,(^2P) + O_2 \rightarrow NO + O \quad \text{(R3)}$$

$$O + NO \rightarrow NO_2 \quad \text{(R4)}$$

$$O + NO_2 \rightarrow NO + O_2 \quad \text{(R5)}$$

These NO and NO_2 are in the gas phase and they can react with •OH to produce nitrous acid (HNO_2) and nitric acid (HNO_3), via reactions (R6) and (R7), which dissolve in the solution leading to a decrease in the pH [18, 44]. Moreover, the NO_2 generated in the gas phase can be dissolved in the aqueous solution to produce dissolved NO_2 in aqueous phase that reacts with the water molecules to produce HNO_3 and HNO_2 (via reaction R8), and finally transform to nitrite (NO_2^-) and nitrate (NO_3^-) (reactions R9 and R10) leading to a decrease in the pH of the treated solution [65]:

$$NO + OH + M \rightarrow HNO_2 + M \quad \text{(R6)}$$

$$NO_2 + OH + M \rightarrow HNO_3 + M \quad \text{(R7)}$$

$$2NO_2 + H_2O \rightarrow HNO_2 + HNO_3 \quad \text{(R8)}$$

$$HNO_2 \rightarrow H^+ + NO_2^- \quad \text{(R9)}$$

$$HNO_3 \rightarrow H^+ + NO_3^- \quad \text{(R10)}$$

(2) The decrease in the pH can be caused by the generation of acidic organics during the decoloration process of MB. To determine the dominant effect in the decrease of the pH obtained in this study, an experiment was conducted for monitoring the change in the pH of pure water treated by the air bubbling plasma at the same operating parameters that were used in the treatment of the MB solution, the results are shown in figure 16. Comparing to the plasma treatment of the pure water, the change of the pH of the organic solution treated by the plasma were more apparent, where the pH of the treated solution is much lower than that of the treated water at the same value of the average power consumed, despite the similar behavior of both cases. Therefore, it is suggested that the degradation of the MB to organic acids has a major role in pH decrease of the treated solution than that of the formation of nitrous and nitric acids. In addition, the results showed that the change in the pH is fairly depended on the initial concentration of the

MB in the treated solution. The higher the initial MB concentration, the lower the pH of the treated solution, where the pH was 4.28 for 5 mg/L of initial MB concentration and 4.18 for 30 mg/L at 5 min of the treatment, and it was 3.94 for 5 mg/L and 3.72 for 30 mg/L at 10 min at the same average power consumed (~ 1.13 W). This indicates that higher organic acids generated at the higher MB concentration.

Figure 15 shows also that the change in the pH of the treated solution depends on the average power consumed, where the pH decreased from 4.8 at average power consumed of 0.42 W to 4.52 at 0.66 W and to 4.4 at 1.13 W at the same treatment time of 5 min. Moreover, it was found that the pH of the treated solution is independent on the conductivity of the solution, where the average of the pH after 12 min of the plasma treatment at 1.13 W of average power consumed and at conductivities of 1, 60, 600 and 1000 μS/cm was 4.15, 4.16, 4.13 and 4.15, respectively.

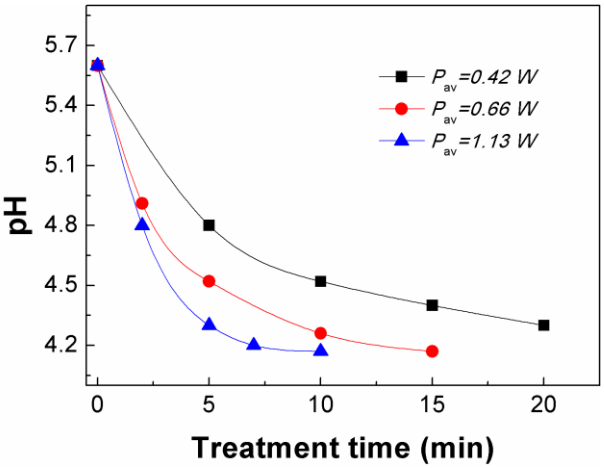

Fig. 15 The pH of the treated solution as a function of the treatment time at different powers and $\sigma_i \approx 1$ μS/cm, f=300 Hz, and C_0=10 mg/L

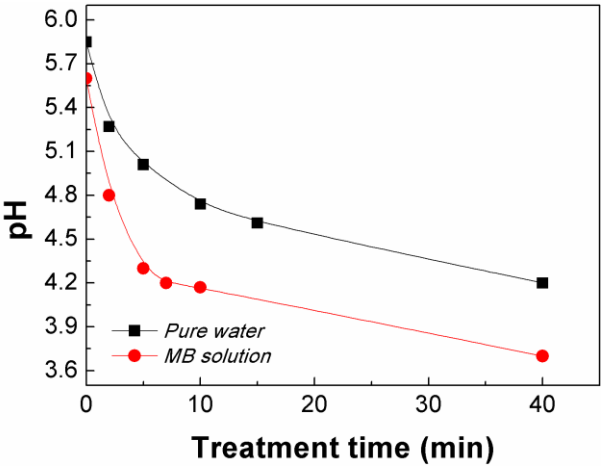

Fig. 16 The pH of the treated deionized water and MB solution as a function of the treatment time and $\sigma_i \approx 1$ μS/cm, f=300 Hz, P_{av}=1.13 W and C_0=10 mg/L

Although the pH and the conductivity of the treated solution have changed remarkably during the treatment time, the solution temperature was almost constant (~ 20 °C) for 60 min of experimental operation. This behavior is matched with that obtained by the plasma treated water surface [65]. Therefore, this experimental result strongly indicates that the input power of discharge is used efficiently to generate reactive species instead of being dissipated as a heat in the system.

4. Conclusions

A simple wire-plate air bubbling plasma discharge based reactor was developed and its ability to decolorate methylene blue as a representative organic pollutant in wastewater was evaluated. The characteristics of the plasma generated in the reactor, the decoloration process of MB, and the main physicochemical properties of the treated solution were investigated. The main results of this study can be summarized as follows:

(1) The plasma generated in the reactor was in the form of filamentary discharge, and it resulted from the PCD and the DBD characteristics of the present reactor..

(2) The effect of the solution conductivity on the power consumed in the reactor was apparent only after a certain applied voltage, when the plasma channels spread in

the bubbles inside the solution. However, the solution conductivity had no role in the decoloration efficiency and the pH of the treated solution at the same input power.

(3) The energy efficiency of the decoloration process increased with increasing the initial concentration of the MB and with decreasing the input power.

(4) First-order kinetics was found suitable to describe the reaction rate of MB decoloration in the air bubbling plasma reactor and the overall first-order reaction rate constant correlated linearly with the average power consumed.

(5) Although the reactor was efficient in the decoloration of the MB, the reduction efficiency of the TOC was still low.

(6) The change in the pH of the treated solution was mainly due to the degradation of MB to acidic byproducts.

(7) There was no increase in the temperature of the solution detected in the reactor during the decoloration process, which indicates that the input power was used effectively to produce reactive species in the reactor instead of dissipating as heat in the system.

Acknowledgements: This work has been conducted at Swansea University and it was financially supported by the Engineering and Physical Sciences Research Council (EPSRC), UK (Grant no. EP/M017141/1). Dr. Ayman would like to thank Assiut University for giving him leave to conduct his postdoctoral research at Swansea University.

Conflict of interest: The authors declare that they have no conflict of interest.

References

[1] I. Panorel, S. Preis, I. Kornev, H. Hatakka, and M. Louhi-Kultanen, "Oxidation of aqueous pharmaceuticals by pulsed corona discharge," *Environ Technol,* vol. 34, pp. 923-30, Mar-Apr 2013.
[2] M. Hijosa-Valsero, R. Molina, H. Schikora, M. Muller, and J. M. Bayona, "Removal of priority pollutants from water by means of dielectric barrier discharge atmospheric plasma," *J Hazard Mater,* vol. 262, pp. 664-73, Nov 15 2013.
[3] B. Jiang, J. Zheng, Q. Liu, and M. Wu, "Degradation of azo dye using non-thermal plasma advanced oxidation process in a circulatory airtight reactor system," *Chemical Engineering Journal,* vol. 204-206, pp. 32-39, 2012.
[4] M. Magureanu, D. Piroi, N. B. Mandache, V. David, A. Medvedovici, and V. I. Parvulescu, "Degradation of pharmaceutical compound pentoxifylline in water by non-thermal plasma treatment," *Water Res,* vol. 44, pp. 3445-53, Jun 2010.
[5] P. Lukes, M. Clupek, V. Babicky, and P. Sunka, "Ultraviolet radiation from the pulsed corona discharge in water," *Plasma Sources Science and Technology,* vol. 17, p. 024012, 2008.
[6] M. Sato, T. Ohgiyama, and J. S. Clements, "Formation of chemical species and their effects on microorganisms using a pulsed high-voltage discharge in water," *IEEE TRANSACTIONS ON INDUSTRY APPLICATIONS,* vol. 32, pp. 106-112, 1996.
[7] W. F. L. M. Hoeben, E. M. v. Veldhuizen, W. R. Rutgers, C. A. M. G. Cramers, and G. M. W. Kroesen, "The degradation of aqueous phenol solutions by pulsed positive corona discharges," *Plasma Sources Science and Technology,* vol. 9, p. 361, 2000.
[8] M. Sato, "degradation of organic contaminants in water by plasma," *International Journal of Plasma Environmental Science & Technology,* vol. 3, pp. 8-14, 2009.
[9] J. Zeng, B. Yang, X. Wang, Z. Li, X. Zhang, and L. Lei, "Degradation of pharmaceutical contaminant ibuprofen in aqueous solution by cylindrical wetted-wall corona discharge," *Chemical Engineering Journal,* vol. 267, pp. 282-288, 2015.
[10] B. Jiang, J. Zheng, S. Qiu, M. Wu, Q. Zhang, Z. Yan*, et al.*, "Review on electrical discharge plasma technology for wastewater remediation," *Chemical Engineering Journal,* vol. 236, pp. 348-368, 2014.
[11] I. Tatsuo, S. Ryota, S. Hiroyasu, and T. Hirotaka, "Refractory organic solute decomposition in water using micowave plasma," *Transactions of the Materials Reserach society of Japan,* vol. 36, pp. 475-478, 2011.
[12] K. Oehmigen, M. Hähnel, R. Brandenburg, C. Wilke, K. D. Weltmann, and T. von Woedtke, "The Role of Acidification for Antimicrobial Activity of Atmospheric Pressure Plasma in Liquids," *Plasma Processes and Polymers,* vol. 7, pp. 250-257, 2010.
[13] N. Lu, J. Li, Y. Wu, and S. Masayuki, "Treatment of Dye Wastewater by Using a Hybrid Gas/Liquid Pulsed Discharge Plasma Reactor," *Plasma Science and Technology,* vol. 14, pp. 162-166, 2012.
[14] P. Bruggeman and C. Leys, "Non-thermal plasmas in and in contact with liquids," *Journal of Physics D: Applied Physics,* vol. 42, p. 053001, 2009.
[15] P. Lukes, M. Clupek, V. Babicky, and P. Sunka, "Pulsed Electrical Discharge in Water Generated Using Porous-Ceramic-Coated Electrodes," *IEEE Transactions on Plasma Science,* vol. 36, pp. 1146-1147, 2008.
[16] H. H. Kim, Y. Teramoto, T. Hirakawa, N. Negishi, and A. Ogata, "Micobubble Formation in Underwater Pulsed Streamer Discharge," *International Journal of Plasma Environmental Science & Technology,* vol. 7, pp. 109-116, 2013.

[17] L. R. Grabowski, E. M. van Veldhuizen, A. J. M. Pemen, and W. R. Rutgers, "Corona Above Water Reactor for Systematic Study of Aqueous Phenol Degradation," *Plasma Chemistry and Plasma Processing,* vol. 26, pp. 3-17, 2006.
[18] Z. He, J. Liu, and W. Cai, "The important role of the hydroxy ion in phenol removal using pulsed corona discharge," *Journal of Electrostatics,* vol. 63, pp. 371-386, 2005.
[19] B. Yang, M. Zhou, and L. Lei, "Synergistic effects of liquid and gas phase discharges using pulsed high voltage for dyes degradation in the presence of oxygen," *Chemosphere,* vol. 60, pp. 405-11, Jul 2005.
[20] M. A. Malik, "Water Purification by Plasmas: Which Reactors are Most Energy Efficient?," *Plasma Chemistry and Plasma Processing,* vol. 30, pp. 21-31, 2009.
[21] K. Takahashi, S. Mukaigawa, K. Takaki, T. Fujiwara, and N. Satta, "water purification using nonthermal plasma driven by blumlein-line stacked pulsed power generator," *J. Plasma Fusion Res. Series,* vol. 8, pp. 1459-1462, 2009.
[22] K. Shimizu, S. Muramatsu, T. Sonoda, and M. Blajan, "Water Treatment by Low Voltage Discharge in Water," *International Journal of Plasma Environmental Science & Technology,* vol. 4, pp. 58-64, 2010.
[23] A. Yamatake, H. Katayama, K. Yasuoka, and S. Ishii, "Water Purification by Atmospheric DC:Pulsed Plasmas inside Bubbles in Water.pdf>," *International Journal of Plasma Environmental Science & Technology,* vol. 1, pp. 91-96, 2007.
[24] X. J. Dai, C. S. Corr, S. B. Ponraj, M. Maniruzzaman, A. T. Ambujakshan, Z. Chen*, et al.*, "Efficient and Selectable Production of Reactive Species Using a Nanosecond Pulsed Discharge in Gas Bubbles in Liquid," *Plasma Processes and Polymers,* vol. 13, pp. 306-310, 2016.
[25] S. Kawano, K. Wada, T. Kakuta, K. Takaki, N. Satta, and K. Takahashi, "Influence of pulse width on decolorization efficiency of organic dye by discharge inside bubble in water," *Journal of Physics: Conference Series,* vol. 441, p. 012007, 2013.
[26] K. Takahashi, I. Yagi, K. Takaki, and N. Satta, "Development of Pulsed Discharge Inside Bubble in Water," *IEEE Transactions on Plasma Science,* vol. 39, pp. 2654-2655, 2011.
[27] M. Sahni and B. R. Locke, "The Effects of Reaction Conditions on Liquid-Phase Hydroxyl Radical Production in Gas-Liquid Pulsed-Electrical-Discharge Reactors," *Plasma Processes and Polymers,* vol. 3, pp. 668-681, 2006.
[28] Y. S. Lee, H. K. Han, and C. Cheong, "Generation of dissolved O3 and OH radicals in water and O3 gas with a submerged low-temperature dielectric barrier discharge plasma reactor " *Journal of environmental biology* vol. 36, pp. 591-595, 2015.
[29] K. Takahashi, K. Takaki, and N. Satta, "Water Remediation Using Pulsed Power Discharge under Water with an Advanced Oxidation Process," *J. Adv. Oxid. Technol.,* vol. 15, pp. 365-366, 2012.
[30] K. Takahashi, Y. Sasaki, S. Mukaigawa, K. Takaki, T. Fujiwara, and N. Satta, "Purification of High-Conductivity Water Using Gas-Liquid Phase Discharge Reactor," *IEEE Transactions on Plasma Science,* vol. 38, pp. 2694-2700, 2010.
[31] L. Zhu, Y. Wang, Z. Ren, G. Liu, and K. Kang, "The Degradation of Organic Pollutants by Bubble Discharge in Water," *Plasma Science and Technology,* vol. 15, pp. 1053-1058, 2013.
[32] A. A. Joshi, B. R. Locke, P. Arce, and W. C. Finney, "Formation of hydroxyl radicals, hydrogen peroxide and aqueous electrons by pulsed streamer corona discharge in aqueous solution," *Journal of Hazardous Materials,* vol. 41, pp. 3-30, 1995.

[33] N. Lu, Y. Feng, J. Li, S. Shang, and Y. Wu, "Electrical Characteristics of Pulsed-Discharge Plasma for Decoloration of Dyes in Water," *IEEE TRANSACTIONS ON PLASMA SCIENCE,* vol. 43, pp. 580-586, 2015.
[34] D. Dobrin, C. Bradu, M. Magureanu, N. B. Mandache, and V. I. Parvulescu, "Degradation of diclofenac in water using a pulsed corona discharge," *Chemical Engineering Journal,* vol. 234, pp. 389-396, 2013.
[35] M. Magureanu, C. Bradu, D. Piroi, N. B. Mandache, and V. Parvulescu, "Pulsed Corona Discharge for Degradation of Methylene Blue in Water," *Plasma Chemistry and Plasma Processing,* vol. 33, pp. 51-64, 2012.
[36] B. R. Locke, M. Sato, P. Sunka, M. R. Hoffmann, and J. S. Chang, "Electrohydraulic Discharge and Nonthermal Plasma for Water Treatment," *Industrial & Engineering Chemistry Research,* vol. 45, pp. 882-905, 2006.
[37] P. Šunka, "Pulse electrical discharges in water and their applications," *Physics of Plasmas,* vol. 8, p. 2587, 2001.
[38] Z. Wang, S. Jiang, and K. Liu, "Treatment of Wastewater with High Conductivity by Pulsed Discharge Plasma," *Plasma Science and Technology,* vol. 16, pp. 688-694, 2014.
[39] B. Dong, J. M. Bauchire, J. M. Pouvesle, P. Magnier, and D. Hong, "Experimental study of a DBD surface discharge for the active control of subsonic airflow," *Journal of Physics D: Applied Physics,* vol. 41, p. 155201, 2008.
[40] A. Abdelaziz, T. Seto, M. Abdel-Salam, and Y. Otani, "Performance of a surface dielectric barrier discharge based reactor for destruction of naphthalene in an air stream," *J. Phys. D: Appl. Phys.,* vol. 45, p. 115201, 2012.
[41] F. D. Baerdemaeker, M. Šimek, J. Schmidt, and C. Leys, "Characteristics of ac capillary discharge produced in electrically conductive water solution," *Plasma Sources Science and Technology,* vol. 16, pp. 341-354, 2007.
[42] M. Magureanu, N. B. Mandache, P. Eloy, E. M. Gaigneaux, and V. I. Parvulescu, "Plasma-assisted catalysis for volatile organic compounds abatement," *Appl. Catal. B: Environ. Sci. Technol.,* vol. 61, pp. 12-20, 2005.
[43] S. A. Smirnov, D. A. Shutov, E. S. Bobkova, and V. V. Rybkin, "Chemical Composition, Physical Properties and Populating Mechanism of Some O(I) States for a DC Discharge in Oxygen with Water Cathode," *Plasma Chemistry and Plasma Processing,* vol. 36, pp. 415-436, 2015.
[44] R. Xiong, A. Nikiforov, P. Vanraes, and C. Leys, "Hydrogen Peroxide Generation by DC and Pulsed Underwater Discharge in Air Bubbles," *J. Adv. Oxid. Technol.,* vol. 15, pp. 197-204, 2012.
[45] P. Manoj Kumar Reddy, B. Rama Raju, J. Karuppiah, E. Linga Reddy, and C. Subrahmanyam, "Degradation and mineralization of methylene blue by dielectric barrier discharge non-thermal plasma reactor," *Chemical Engineering Journal,* vol. 217, pp. 41-47, 2013.
[46] M. Magureanu, D. Piroi, F. Gherendi, N. B. Mandache, and V. Parvulescu, "Decomposition of Methylene Blue in Water by Corona Discharges," *Plasma Chemistry and Plasma Processing,* vol. 28, pp. 677-688, 2008.
[47] R. Zhang, C. Zhang, X. Cheng, L. Wang, Y. Wu, and Z. Guan, "Kinetics of decolorization of azo dye by bipolar pulsed barrier discharge in a three-phase discharge plasma reactor," *J Hazard Mater,* vol. 142, pp. 105-10, Apr 2 2007.
[48] H. Wu, Z. Fang, T. Zhou, C. Lu, and Y. Xu, "Discoloration of Congo Red by Rod-Plate Dielectric Barrier Discharge Processes at Atmospheric Pressure," *Plasma Science and Technology,* vol. 18, pp. 500-505, 2016.

[49] A. Abdelaziz, T. Ishijima, T. Seto, N. Osawa, H. Wedaa, and Y. Otani, "Characterization of surface dielectric barrier discharge influenced by intermediate frequency for ozone production," *Plasma Sources Sci. Technol.,* vol. 25, p. 035012, 2016.
[50] F. Huang, L. Chen, H. Wang, and Z. Yan, "Analysis of the degradation mechanism of methylene blue by atmospheric pressure dielectric barrier discharge plasma," *Chemical Engineering Journal,* vol. 162, pp. 250-256, 2010.
[51] L. Chandana, P. Manoj Kumar Reddy, and C. Subrahmanyam, "Atmospheric pressure non-thermal plasma jet for the degradation of methylene blue in aqueous medium," *Chemical Engineering Journal,* vol. 282, pp. 116-122, 2015.
[52] L. R. Grabowski, E. M. v. Veldhuizen, A. J. M. Pemen, and W. R. Rutgers, "Breakdown of methylene blue and methyl orange by pulsed corona discharge," *Plasma Sources Science and Technology,* vol. 16, pp. 226-232, 2007.
[53] B. Wang, B. Sun, X. Zhu, Z. Yan, Y. Liu, and H. Liu, "Degradation of Methylene Blue by Microwave Discharge Plasma in Liquid," *Contributions to Plasma Physics,* vol. 53, pp. 697-702, 2013.
[54] X. Liu, H. Zhang, D. Qin, Y. Yang, Y. Kang, F. Zou*, et al.*, "Radical-Initiated Decoloration of Methylene Blue in a Gas–Liquid Multiphase System Via DC Corona Plasma," *Plasma Chemistry and Plasma Processing,* vol. 35, pp. 321-337, 2015.
[55] S. D. Anghel, D. Zaharie-Butucel, and I. E. Vlad, "Single electrode Ar bubbled plasma source for methylene blue degradation and concurrent synthesis of carbon based nanoparticles," *Journal of Electrostatics,* vol. 75, pp. 63-71, 2015.
[56] C. Tizaoui and N. Grima, "Kinetics of the ozone oxidation of Reactive Orange 16 azo-dye in aqueous solution," *Chemical Engineering Journal,* vol. 173, pp. 463-473, 2011.
[57] Y. Wu, J. Li, G. F. Li, N. Li, G. Z. Qu, C. H. Sun*, et al.*, "Decomposition of Phenol in Water by Gas Phase Pulse Discharge Plasma," in *Industry Applications Society Annual Meeting, 2009. IAS 2009. IEEE*, 2009, pp. 1-4.
[58] H. Wu, Z. Fang, and Y. Xu, "Degradation of Aniline Wastewater Using Dielectric Barrier Discharges at Atmospheric Pressure," *Plasma Science and Technology,* vol. 17, pp. 228-234, 2015.
[59] Y. Zhang, X. Xiong, Y. Han, H. Yuan, S. Deng, H. Xiao*, et al.*, "Application of titanium dioxide-loaded activated carbon fiber in a pulsed discharge reactor for degradation of methyl orange," *Chemical Engineering Journal,* vol. 162, pp. 1045-1049, 2010.
[60] D. R. Grymonpre, A. K. Sharma, W. C. Finney, and B. R. Locke, "The role of Fenton's reaction in aqueous phase pulsed streamer corona reactors," *Chemical Engineering Journal,* vol. 82, pp. 189-207, 2001.
[61] Q. Tang, W. Jiang, Y. Zhang, W. Wei, and T. M. Lim, "Degradation of Azo Dye Acid Red 88 by Gas Phase Dielectric Barrier Discharges," *Plasma Chemistry and Plasma Processing,* vol. 29, pp. 291-305, 2009.
[62] L. Gao, L. Sun, S. Wan, Z. Yu, and M. Li, "Degradation kinetics and mechanism of emerging contaminants in water by dielectric barrier discharge non-thermal plasma: The case of 17β-Estradiol," *Chemical Engineering Journal,* vol. 228, pp. 790-798, 2013.
[63] J. Xue, L. Chen, and H. Wang, "Degradation mechanism of Alizarin Red in hybrid gas–liquid phase dielectric barrier discharge plasmas: Experimental and

theoretical examination," *Chemical Engineering Journal,* vol. 138, pp. 120-127, 2008.
[64] Y. Huang, Y. Kou, C. Zheng, Y. Xu, Z. Liu, and K. Yan, "Escherichia Coli Inactivation in Water Using Pulsed Discharge," *IEEE Transactions on Plasma Science,* vol. 44, pp. 938-943, 2016.
[65] K. Shang, J. Li, X. Wang, D. Yao, N. Lu, N. Jiang*, et al.*, "Evaluating the generation efficiency of hydrogen peroxide in water by pulsed discharge over water surface and underwater bubbling pulsed discharge," *Japanese Journal of Applied Physics,* vol. 55, p. 01AB02, 2016.